CHEMISTRY
A European Journal

A Journal of
ChemPubSoc Europe

Accepted Article

Title: Hydrating the Bispropionate Notch in Malaria Pigment: A New Structural Motif in the Iron(III)(deuteroporphyrin) Dimer.

Authors: david kuter, liliana suarez, bruce c noll, erin l dodd, peter w stephens, and Scott Bohle

To be cited as: *Chem. Eur. J.* 10.1002/chem.201805116

Link to VoR: http://dx.doi.org/10.1002/chem.201805116

Supported by
ACES

WILEY-VCH

10.1002/chem.201805116

Hydrating the Bispropionate Notch in Malaria Pigment: A New Structural Motif in the Iron(III)(deuteroporphyrin) Dimer.

David Kuter[a,d], Liliana Suárez[a], Erin L. Dodd[a], Bruce C. Noll[c], Peter W. Stephens[*b], and D. Scott Bohle[*a]

[a] Department of Chemistry, McGill University, 801 Sherbrooke St. W., Montreal H3A 0B8 CANADA; [b]Department of Physics and Astronomy, State University of New York, Stony Brook, Stony Brook New York, 11794-3800 USA; [c]Bruker-AXS, 5465 E Cheryl Pkwy, Fitchburg, WI 53711, USA; [d]Department of Chemistry and Polymer Science, Stellenbosch University, Private Bag X1, Matieland, 7602, Stellenbosch, South Africa.

Abstract: Treating deuterohemin, chloro(deuteroprophyrinato)iron(III), with a non-coordinating base in DMSO and methanol allows for the isolation of [(deuteroporphyrinato)iron(III)]$_2$, deuterohematin anhydride (DHA), an analog of malaria pigment, the natural product of heme detoxification by malaria. The structure of DHA from this solvent system has been solved by X-ray powder diffraction and displays many similarities and important structural differences with malaria pigment. Most notably a water of solvation occupies a notch created by the propionate sidechains and stabilizes a markedly bent propionate coordinated with a long Fe-O bond and the formation of carboxylate cluster associated with the waters. Together these account for its increased solubility and more open structure with an increased porphyrin-porphyrin separation. The IR spectroscopic signature associated with this structure also accounts for the strong IR bands at 1587 cm^{-1} which are present in many amorphous preparations of synthetic malaria pigment and it is proposed that stabilizing these structures may be new motif to target antimalarial drugs. The important role for the vinyl substituents in this biochemistry is further demonstrated by the structure of deuterohemin from single crystal X-ray diffraction.

10.1002/chem.201805116

Introduction In a brief synchronized timeline, the malaria parasite repeatedly invades human red blood cells, imports hemoglobin into a digestive vacuole, degrades the hemoglobin peptides, oxidizes the heme to iron(III), and crystallizes the resulting Fe(III)(protoporphyrinato) molecule into the excretion product known as malaria pigment.[1] This unique biochemistry presents many of the known[2,3] drug targets for past and future generations of antimalarials and all are the subject of sustained intense investigation.[4,5] While some aspects of this time line are now well understood, particularly the molecular and structural biology of the peptidases which degrade hemoglobin,[6-8] other processes[9,10] such as heme oxidation, heme transport, and heme crystallization remain poorly understood.[11] Even the ultimate product of heme crystallization, malaria pigment, also termed hemozoin (HZ), has aspects of its structural and surface chemistry still to be resolved.[12]

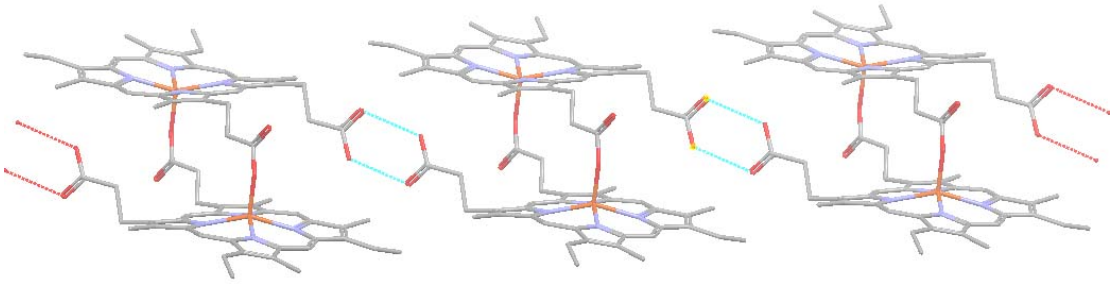

Figure 1 Propionic acid structural roles in HZ and HA, [Fe(protoporphyrinato)]$_2$. Each heme has one Fe-O bond to one propionate and the second propionic acid forms a H-bonded dimer. H-bonds are shown as blue or red dashed lines with a conventional CPK atomic coloring scheme employed. Structure shown taken from the CDC entry XETXUP and shows only one set of positions for the disordered vinyl groups.[13]

A particularly challenging problem in the biosynthesis of HZ is its remarkable crystallinity and the rate at which a single phase crystallizes from the heterogeneous milieu of the digestive vacuole.[14] Following its original structural elucidation by X-ray powder diffraction in 2000,[13] there have been four separate powder diffraction structure determinations[15-17] as well as single crystal structures of a DMSO solvated phase.[18] In each case, either synthetic (hematin anhydride, HA[§])[13,15,16,18,19] or natural (HZ),[17] the structure consists of iron(III)(protoporphyrinato) dimers. The reported variations in structural models are solely related to the presence/absence of solvent interrupting the H-bonded propionic acid chain, and differing models for the vinyl disorder. Thus, regardless of source, natural or synthetic, HA and HZ are isostructural and have the base structure shown in Figure 1, a chain of propionate linked dimers. Inhibiting the formation of HZ is the consensus drug target for the quinoline family of antimalarials.[5,20] There has been a sustained effort to synthetically mimic and inhibit this crystallization step and one resulting general observation is that unless crystallization is slowed with a competing solvolysis, by performing the reaction in DMSO for example,[21] substantial amounts of amorphous products are obtained. Thus, synthetic HA is usually contaminated to varying degrees by other amorphous phases characterized by strong IR bands at 1585 cm^{-1} in addition to those at 1712 and 1664 cm^{-1} in HZ and purified HA.[22] The malaria parasite avoids the formation of these amorphous phases by an as yet unknown mechanism. In synthetic materials, these amorphous phases are usually treated as a nuisance and their higher solubility/reactivity is exploited in subsequent vigorous purification/washing steps with bicarbonate buffer, pyridine, water and methanol. In many conditions, these amorphous phases are the main product of the reaction and once posed severe limitations on early efforts to structurally characterize HA with X-ray diffraction.[23] To date, little is known of these materials apart from their unique IR signature, their reactivity/solubility

10.1002/chem.201805116

and their lack of crystallinity. In this contribution we present a structure of a related phase of HA, with deuteroporphyrin instead of protoporphyrin, which has the IR signature and reactivity/solubility of these amorphous phases. We propose that this new variant of the HZ structure/motif adds to our understanding of heme crystallization in HZ and may ultimately aid in the development of new antimalarials.

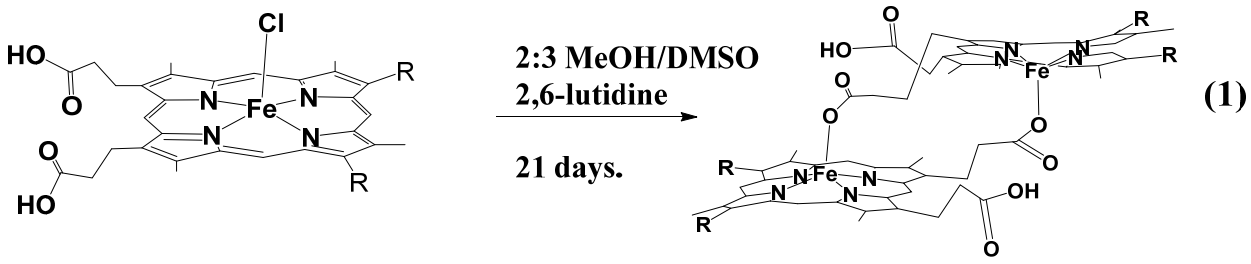

(1)

R= CH=CH$_2$; Hemin
R = H; Deuterohemin, DH

R= CH=CH$_2$; Hematin anhydride, HA
R = H; Deuterohematinanhydride, DHA

Results and Discussion

Deuterohematin anhydride, DHA, the deuteroporphyrin devinylated analog of HA, is prepared by the dehydrohalogenation of deuterohemin, DH, with a non-coordinating base, 2,6-lutidine (equation 1).[15] Solvent effects are important in these transformations with other solvents and bases leading to different semi-crystalline materials, Figure S6.[24] The structure of the DMSO/MeOH product was solved as a hydrate from synchrotron powder diffraction data, Figures 2, 3, S3, with Figure S2 showing the diffraction pattern and refined final Rietveld fit. As shown in Figure 2A, the deuteroporphyrin forms an inversion related dimer pair. Thus, as with HZ, Figure 1, DHA shares the common η^1 iron bound propionate bound dimer with the iron 0.5 Å out of the plane of the porphyrin and displaced towards the propionate ligand. It does not, however, form a chain of propionic H-bonded dimers. Further refinement details are given in the

10.1002/chem.201805116

Table S1 and S6 with a detailed contrast of HA and DHA is given in Table S5. Also shown in Figure S1 and Table S5 are related bispropionate linked dimers.

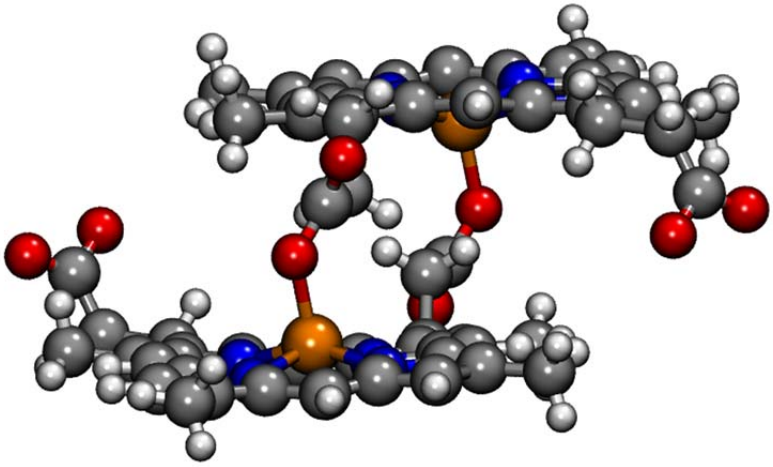

(A)

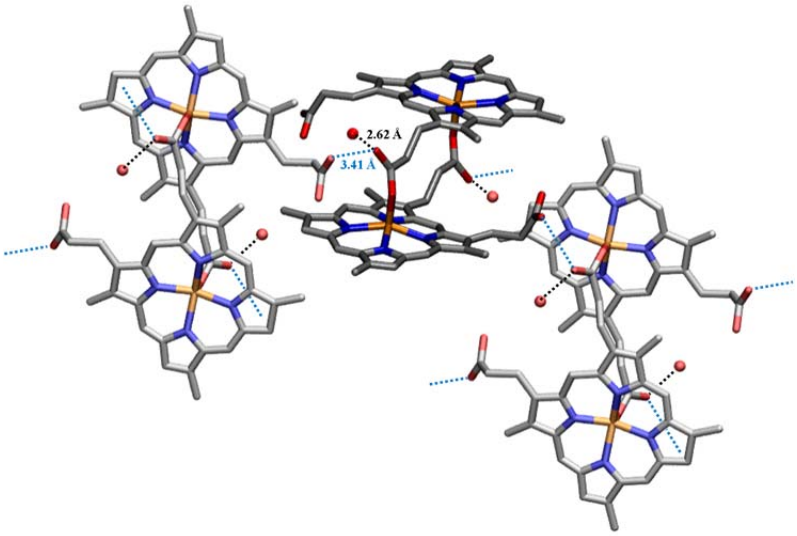

(B)

Figure 2. Structure of DHA. **(A)** Tilting of the intradimer pair in DHA, hydrates not shown. **(B)** Packing of propionate linked dimers showing H-bonds (black dashed lines) and close contacts (blue dashed lines) between free propionic acid and non-iron bound propionate oxygen. Note the water occupying the gap or notch between the two propionic acid side chains.

While the structures of HA and DHA share similarity in being comprised of inversion dimers for the iron and porphyrin core, there are notable differences in their hydration, intra-dimer geometry, the inter-dimer interactions, as well as crystallographic symmetry. Within the dimer of DHA, the iron carboxylates are tilted or canted by 61.0° away from the orthogonal orientation found in HA and in many metallocarboxylates.[25] This tilt is accompanied by an increase in the iron-oxygen bond length to 1.94(7) Å, an increase in the separation of the porphyrin planes to 4.82 Å, and a lateral offset of the porphyrins by 4.47 Å. Additionally, there is almost no overlap of the two intra-dimer porphyrin planes. One result of this "opening up" of the structure is that it allows for the most unusual feature of the DHA structural motif – the formation of a hydrated carboxylic acid cluster with weak H-bonds between free propionic acid groups on neighboring dimers as well as the hydrate to the non-iron bound oxygen of the coordinated propionate. The later O---[H]---O separation of 2.614 Å, suggests that the iron bound propionate ligand could be described as an oxygen coordinated propionic acid derivative. The collected structure of the two propionates, two propionic acids, and two waters is shown schematically in Figure 3. This unusual H-bonded cluster accounts for many of the structural changes found in DHA. Remarkably this crystallographic structure is closely related to the optimized DFT geometry for a hydrated dimer, Table 1 and Figures S8. The structural contrast of HA and DHA structural motifs illustrates some of key interactions within the propionate bonding of the dimer. As shown in Figures 3 and S4 the two parallel propionates in HA adopt a more open and kinked arrangement characterized by the torsion angles in Table S5. The contrast of the free and the metal bound propionates in HA and DHA is

10.1002/chem.201805116

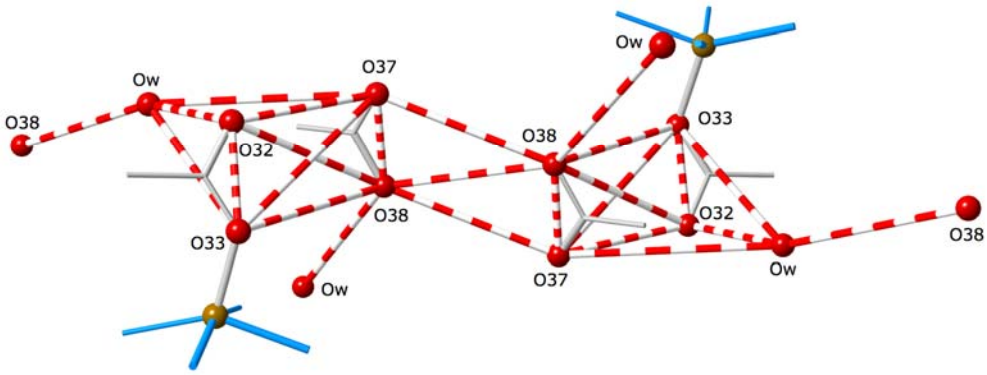

Figure 3 Water and carboxylate cluster in DHA. Oxygens from four different propionates are shown as red spheres O32, O33, O37 and O38 and two water as Ow. In grey are the carboxylate carbons and in blue the Fe-N bonds to the two deuterohemes. Iron atoms are depicted in brown/rust-orange.

seen in the similarity of the conformation of the metal bound group while in free propionate large differences of 90°, 100°, and 40° are seen in the respective torsion angles of the two structures. The gap created by the propionates in HA provides a notch or a groove for a neighboring iron bound propionate to pack closely in the lattice with key metric parameters collected in Table 1. In DHA this site is blocked by the water of hydration and the resulting carboxylates form the cluster shown in Scheme S1 and Figure S3. This key site is also occupied by the side chain of chloroquine, CQ, in the crystal structure of the model gallium analog, [Ga(protoporphyrinato)(OMe)]$_2$·CQ$_2$,[26] and this site also exhibits significant porphyrin/drug interactions by NOESY/NMR studies in solution.[27] Perhaps most importantly of all in the structure of HA/HZ this site is filled by the propionate of an adjacent heme dimer and in the single crystal structure of the DMSO solvate of HA the one of the DMSO methyl groups is at the

10.1002/chem.201805116

entrance to this notch.[18] The bispropionate notch is an important drug target of the heme/antimalarial drug binding interaction.

Table 1 Metrical Parameters of the Propionate Notch

Structure	HA	[Ga(PP)]$_2$.2CQ	DHA·2H_2O Experimental	DHA·H_2O Mono-Theory	DHA·2H_2O Di-Theory
CCDC Code	XETXUP	DONRAB	This work	B3LYP/cc-pvdz[#]	B3LYP/cc-pvdz[#]
	162267	904065			
Metric					
O-------O (Å)[a]	6.94	6.44	7.38	5.00	5.00, 5.00
C-------C (Å)[b]	6.65	6.46	8.05	5.85	5.95, 5.95
X[c]	(C)==O	CH_2	H_2O	H_2O	H_2O
X-----O (Å)[d]	3.65, 4.14	2.50, 2.93	2.62, 4.91	2.83; 3.03	2.82, 3.05 2.82, 3.04
X-----HC_m (Å)[e]	4.85	4.02	3.16	2.34	2.36, 2.36
O--X--O (°)[f]	153.0	130.9	159.3	117.4	116.95,116.95
C--X--C (°)[g]	173.8	103.5	143.2	120.7	120.80,120.79
M-O (Å)[h]	1.893	2.007	1.945	1.881; 1.852	1.880, 1.880
M--O--O (°)[i]	166.5	168.1	143.8	140.7;162.5	134.65, 134.65

[#]Stationary points for hydrates with two high spin heme for the gas phase B3LYP/cc-pvdz.

[a] Closest propionate oxygen atom separation; [b] Separation of propionate carbons; [c] Functional group held in notch. –C(O)-OFe oxygen of HA, a methylene of CQ in its gallium adduct, and the water of the DHA solvate. [d] X-oxygen separations for propionates that define the notch. For each pair listed the first and the shorter distance corresponds to the distance to the iron bound oxygen, and the second to FeOC=**O**; [e] The X ---H separation for the proton on the C_m between pyrroles C and D; [f] O-X-O angle for the propionate oxygens, and [g] The C-X-C angle for the propionate carbons. [h,i] Fe-O given for the water bound propionate pair and the water free pair of propionates.

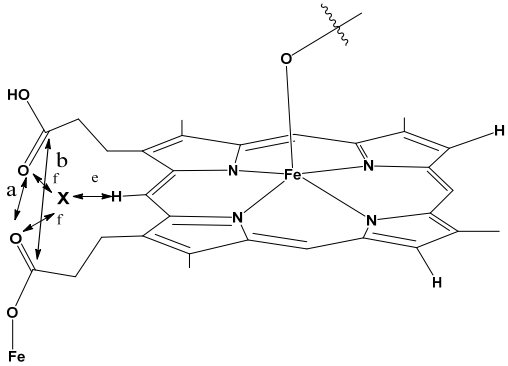

10.1002/chem.201805116

Vibrational spectroscopy remains one of the best tools for deciphering the propionic acid interactions in the heme family of condensed phases[15,28] and the structure of DHA provides a valuable new reference point for this technique. As shown in Figure 4, the IR spectrum of DHA has strong propionic sidechain bands at 1729, 1654, 1587, and at 1206 cm^{-1}. All of these bands correspond well with bands present in the IR spectrum of HA prepared without extensive purification/washing (crude HA), Figure 4A. However, on purification, the feature at 1584 $cm^{-1}$is lost (Figure 4B). This behavior is in contrast to DHA, where the 1587 cm^{-1} band persists even after extensive bicarbonate washes during its work up. Many preparations of synthetic HA have similar bands at ~1585 cm^{-1} upon their initial isolation, but these are lost (along with much of the product!) during the subsequent workup steps. We propose that this band is diagnostic of the type of bonding depicted in Figure 3, that is with a partial formal structure of $–CH_2$-C(OH)=O-Fe, with its relative durability being due to it being an integral part of the lattice. It is significant that in biomimetic syntheses of HA, as well as in hemozoin isolated from the parasite, that this

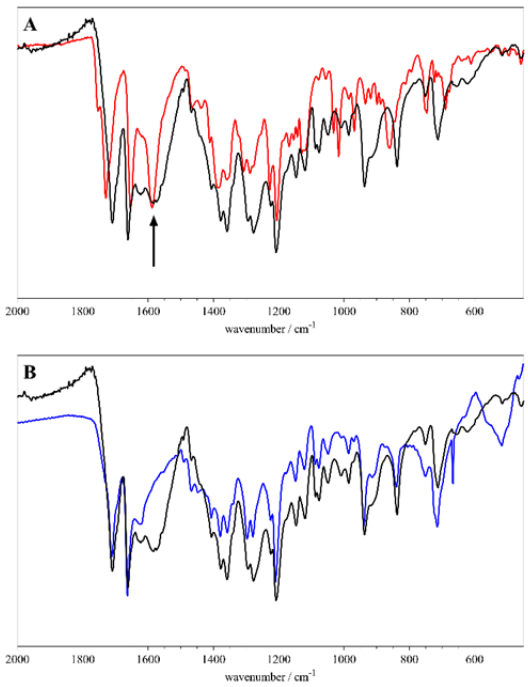

Figure 4. IR spectra of DHA and HA. (**A**) DHA (red) versus crude HA (black); and (**B**) Extensively washed HA (blue) versus crude HA (black). Spectra measured with a diamond cell ATR and show the common strong carboxyl band at 1587 cm^{-1} (black arrow) which is present in DHA and crude HA. The band 1584 cm^{-1} is absent in purified HA.

band has little, if any, intensity. Additional support for this assignment is from the B3LYP/cc-pvdz calculated gas phase vibrational modes for the HA dimer with pendant propionic acids and the DHA internally bonded bent propionic acids, Figure S9 and Table S8. Here there is a net decrease in the carboxylate stretching modes by ~ 90 cm^{-1} for the DHA structure. Further theoretical studies of the hydrated model are underway. The implication is that the parasite prevents these types of interactions from forming or, if formed, from propagating in the final product. DHA is much more soluble than HA, and HA/HZ crystallinity and insolubility may stem from the absence of these interactions as well as the converse that poorly aggregated/crystallized synthetic HA has a large fraction of these phases. We note that the structure of DHA is more consistent with spectroscopic results than prior trimeric and polymeric models proposed for these phases.[29]

Clearly the two vinyl substituents in protoporphyrin are an important factor in controlling the HZ crystallization and phase selectivity.[30,31] Similar considerations are also found in the structural biology of heme proteins where both the propionic acids on one side of the porphyrin as well as the two vinyl group on the opposing side orient the heme with its binding pocket.[30,31] To further understand the structural role of the vinyl groups in hemin chemistry, we have also structurally characterized deuterohemin (DH), the starting material of DHA synthesis. This readily accessible derivative is obtained by a resorcinol thermolytic vinyl cleavage from Fe(III)(protoporphyrinato)chloride, hemin, Figure S5.[32] As shown in Figure 5, the absence of the two vinyl groups at carbon atoms C(13) and C(16) does not appear to markedly influence the porphyrin and iron geometry. However, when compared to its hemin precursor, the intermolecular packing arrangement in the solid state is markedly affected. In DH, the hydrogen bonding between the propionic acids leads to an offset chain, Figure 5A, whereas in hemin (not

shown) the propionic acids form a simple dimer with another single hemin. This offset chain propagates along the crystallographic 2_1 screw axis present in DH but is absent in the P-1 lattice of hemin.

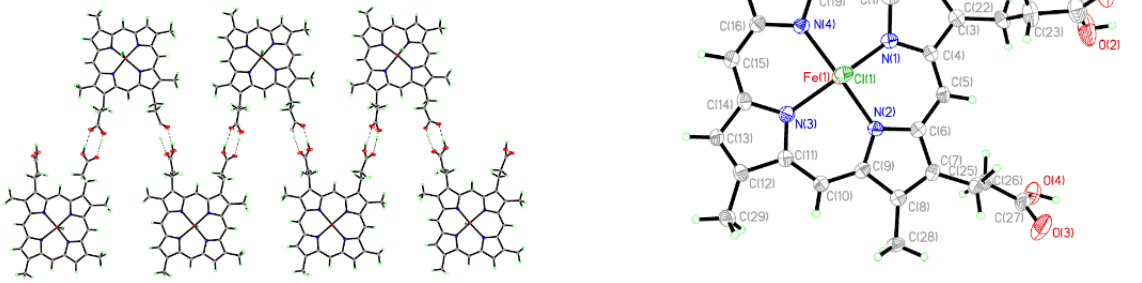

(A) **(B)**

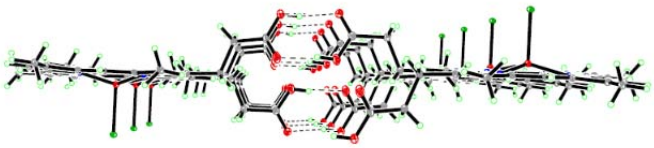

(C)

Figure 5. (A) Single crystal X-ray diffraction structure of the deuteroheme in DH viewed down the Cl-Fe axis. Intermolecular interactions in DH viewed **(B)** perpendicular to and **(C)** along the 2/1 screw axis.

Conclusion

The structure of DHA in Figure 2 suggests an important new approach or motif the design of antimalarial drugs. Numerous computational and synthetic efforts have focused on the putative

drug targets on the faces of the growing hemozoin crystal.[33-38] However, on the other side of the equilibrium are heme dimers in solution, either linked by propionates, μ-oxo-bridges, or by London dispersive forces[14] and if these can be stabilized, then heme sequestration and detoxification will also be disrupted. Alternatively, if heme precipitation can be directed towards DHA-like phases and away from the HA structure then there may also be increased solubility of the heme. Either mechanism might in principle accomplish the same net result: parasite homeostasis and diminished proliferation leading to decreased parasitemia in the host. As the pressing need for new antimalarials becomes ever more critical,[39] the new structural motif of DHA represents a complimentary new approach to the extensive efforts currently underway to control malaria.

Competing Interests

The authors declare no competing interests.

Author Contributions

DSB and PWS conceived the study, PWS and BCN measured the diffraction data and solved the powder and single crystal structures respectively. DSB and DK performed density functional studies, ELD, LS, and DK performed the experiments, and analyzed the data. DSB, PWS, DK, ELD, and LS wrote the manuscript with input from all authors.

Acknowledgments

We gratefully acknowledge support from the Burroughs Wellcome Fund, NSERC, FQRNT, and CRC. DK acknowledges the South African NRF for funding. Use of the National Synchrotron

Light Source, Brookhaven National Laboratory, was supported by the U.S. Department of Energy, Office of Basic Energy Sciences, under Contract No. DE-AC02-98CH10886.

Methods

Crystallography: Synchrotron powder X-ray diffraction (SPXD) data were collected at ambient temperature the National Synchrotron Light Source (NSLS), Brookhaven National Laboratory. Diffraction data analysis and Rietveld refinement were performed with TOPAS-Academic.[40] The diffraction pattern was indexed to a monoclinic cell, and the structure was solved using simulated annealing. Details are given in Table S1. In the Rietveld refinement, restraints based on literature values of similar iron porphyrins were placed on bond distances and angles, and on the planarity of the porphyrin moiety. However, no restraints were placed on the position of the Fe atom or the geometry of the axial Fe-O bond. The Rietveld refinement is shown in Figure S2 and the structure is illustrated in Figure 2 of the main text. The data is available from the CCDC 1494078.

Single Crystal diffraction: Dark red plate-like crystals of $C_{30}H_{28}ClFeN_4O_4$ were obtained from slow evaporation from a chloroform solution. The crystal selected had the approximate dimensions 0.040 mm x 0.090 mm x 0.210 mm, was used for the X-ray crystallographic analysis. The X-ray intensity data were measured on a Bruker PROSPECTOR diffractometer system equipped with a multilayer mirror monochromator and a Cu $K_{\alpha 1}$ microfocus sealed tube (λ = 1.54178 Å). The data is available from the CCDC 1868333.

Theoretical Methods: The optimized gas phase structures of the non-hydrated dimers for HA and DHA were calculated using density functional theory, B3LYP/cc-pvdz, with the experimental structures as starting points. Both correspond to local minima with all positive vibrational modes. The optimized structures are shown in Figure S9 and the key vibrational modes collected in Table S8. All of the calculations described above were performed using

Gaussian 98.[41] Computations were carried out at the restricted Hartree-Fock (RHF),[42] and Density Functional Theory (DFT) levels .

Supporting Information Supporting information is available online. The structures of deuterohemin chloride and deuterohematin anhydride have been deposited with the Cambridge Crystallographic Data Centre, acquisition numbers 1471969 and 1494079 respectively.

[§] The nomenclature of the Fe(III)(porphyrin) materials is poorly consolidated. For the protoporphyrin family Fe(III)(PP)X are named hemin when X = chloride, and α–hematin with X = OH. The phase present in malaria pigment, HZ, has X = propionate but the synthetic material is often incorrectly referred to as β-hematin, that is the second isomeric phase of hematin. In analogy with the anhydrides of the carboxylic and sulfonic acids we term the propionate dimer phases as anhydrides; thus hematin anhydride is HA. By analogy the synthetic related material of deuteroporphyrin is DHA, deuterohematin anhydride. Ferriprotoporphyrin anhydride has also been suggested as a better name than β-hematin.

References

(1) Wunderlich, J.; Rohrbach, P.; Dalton, J. P. The malaria digestive vacuole. *Front. Biosci., Scholar Ed.* **2012**, *S4*, 1424-1448.

(2) White, J.; Tathod, P. K. Indispensible malaria genes. *Science* **2018**, *360*, 490-491.

(3) Zhang, M., Wang, C., Otto, T.D., Oberstaller, J.; Liao, X.; Adapa, S.R.; Udenze, K.; Bronner, I.F., Casandra, D.; Mayho, M.; Brown, J.; Li, S.; Swanson, J.; Adams, J.H. Uncovering the essential genes of the human malaria parasite *Science* **2018**, *360*, 506.

(4) de Villiers, K. A.; Egan, T. J. Iron(III) protoporphyrin IX and hemozoin: key targets in the chemotherapy of malaria. *Handb. Porphyrin Sci.* **2014**, *27*, 211-254.

(5) Sullivan, D. J., Jr. Quinolines block every step of malaria heme crystal growth. *Proc. Natl. Acad. Sci. U. S. A.* **2017**, *114*, 7483-7485.

(6) Sigala, P. A.; Goldberg, D. E. The peculiarities and paradoxes of Plasmodium heme metabolism. *Annu. Rev. Microbiol.* **2014**, *68*, 259-278.
(7) Ke, H.; Sigala, P. A.; Miura, K.; Morrisey, J. M.; Mather, M. W.; Crowley, J. R.; Henderson, J. P.; Goldberg, D. E.; Long, C. A.; Vaidya, A. B. The heme biosynthesis pathway is essential for Plasmodium falciparum development in mosquito stage but not in blood stages. *J. Biol. Chem.* **2014**, *289*, 34827-34837, 34812 pp.
(8) Goldberg, D. E. Complex nature of malaria parasite hemoglobin degradation. *Proc. Natl. Acad. Sci. U. S. A.* **2013**, *110*, 5283-5284.
(9) Olafson, K. N.; Nguyen, T. Q.; Rimer, J. D.; Vekilov, P. G. Antimalarials inhibit hematin crystallization by unique drug-surface site interactions. *Proc. Natl. Acad. Sci. U. S. A.* **2017**, *114*, 7531-7536.
(10) Sandlin Rebecca, D.; Fong Kim, Y.; Carrell Holly, M.; Wright David, W.; Wicht Kathryn, J.; Egan Timothy, J. Identification of β-hematin inhibitors in a high-throughput screening effort reveals scaffolds with in vitro antimalarial activity. *Int J Parasitol Drugs Drug Resist* **2014**, *4*, 316-325.
(11) Dodd Erin, L.; Bohle, D. S. Orienteening the Heterocyclic Periphery: a structural model for chloroquine's antimalarial activity *Chem. Commun.* **2014**, *50*, 13765-13768.
(12) Guerra, E. D.; Bohle, D. S.; Cerruti, M. Surface Characterization of Hematin Anhydride: A Comparison between Two Different Synthesis Methods. *Langmuir* **2016**, *32*, 4479-4484.
(13) Pagola, S.; Stephens, P. W.; Bohle, D. S.; Kosar, A. D.; Madsen, S. K. The structure of malaria pigment b-haematin. *Nature (London)* **2000**, *404*, 307-310.
(14) Kuter, D.; Streltsov, V.; Davydova, N.; Venter, G. A.; Naidoo, K. J.; Egan, T. J. Molecular Structures and Solvation of Free Monomeric and Dimeric Ferriheme in Aqueous Solution: Insights from Molecular Dynamics Simulations and Extended X-ray Absorption Fine Structure Spectroscopy. *Inorg. Chem.* **2014**, *53*, 10811-10824.
(15) Bohle, D. S.; Dodd, E. L.; Stephens, P. W. Structure of Malaria Pigment and Related Propanoate-Linked Metalloporphyrin Dimers. *Chem. Biodiversity* **2012**, *9*, 1891-1902.
(16) Straasø, T.; Kapishnikov, S.; Kato, K.; Takata, M.; Als-Nielsen, J.; Leiserowitz, L. The Role of the Four Stereoisomers of the Heme Fe-O Cyclic Dimer in the Crystalline Phase Behavior of Synthetic Hemozoin: Relevance to Native Hemozoin Crystallization. *Cryst. Growth Des.* **2011**, *11*, 3342-3350.
(17) Klonis, N.; Dilanian, R.; Hanssen, E.; Darmanin, C.; Streltsov, V.; Deed, S.; Quiney, H.; Tilley, L. Hematin-Hematin Self-Association States Involved in the Formation and Reactivity of the Malaria Parasite Pigment, Hemozoin. *Biochem.* **2010**, *49*, 6804-6811.
(18) Gildenhuys, J.; Roex, T. l.; Egan, T. J.; deVilliers, K. A. The Single Crystal X-ray Structure of β-Hematin DMSO Solvate Grown in the Presence of Chloroquine, a β-Hematin Growth-Rate Inhibitor. *J. Am. Chem. Soc.* **2013**, *135*, 1037-1047.
(19) Bohle, D. S.; Dodd, E. L.; Kosar, A. J.; Sharma, L.; Stephens, P. W.; Suarez, L.; Tazoo, D. Soluble Synthetic Analogues of Malaria Pigment: Structure of Mesohematin Anhydride and its Interaction with Chloroquine in Solution. *Angew. Chem. Int. Ed.* **2011**, *50*, 6151-6154.
(20) Chong, C. R.; Sullivan, D. J. Inhibition of heme crystal growth by antimalarials and other compounds: implications for drug discovery. *Biochemical Pharmacology* **2003**, *66*, 2201-2212.
(21) Bohle, D. S.; Helms, J. B. Synthesis of β-hematin by dehydrohalogenation of hemin. *Biochem. Biophys. Res. Commun.* **1993**, *193*, 504-508.
(22) Slater, A. F.; Swiggard, W. J.; Orton, B. R.; Flitter, W. D.; Goldberg, D. E.; Cerami, A.; Henderson, G. B. An iron-carboxylate bond links the heme units of malaria pigment. *Proc. Nat. Acad.Sci.(USA)* **1991**, *88*, 325-329. .
(23) Bohle, D. S.; Kosar, A. D.; Stephens, P. W. Phase homogenity and crystal morphology of the malaria pigment β-hematin. *Acta Crystallogr., Sect. D, Biol. Crystallog.* **2002**, *D58*, 1752-1756.

(24) Bohle, D. S.; Kosar, A. D.; Stephens, P. W. Phase homogeneity and crystal morphology of the malaria pigment b-hematin. *Acta Cryst. Sec. D: Biol. Cryst.* **2002**, *D58*, 1752-1756.
(25) Herold, S.; Lippard, S. J. Carboxylate-Bridged Diiron(II) Complexes. *J. Am. Chem. Soc.* **1997**, *119*, 145-156.
(26) Bohle, D. S.: Dodd, E. L.; [Gallium(III) protoporphyirin IX]$_2$: A soluble Diamagnetic Model for Malaria Pigment. *Inorg. Chem.* **2012**, *51*, 4411-4413.
(27) Dodd, E. L. T., D.; Bohle, D. S. Solution and Solid State Correlations of Antimalarial Drug Actions: NMR and Crystallographic Studies of Drug Interactions with a Heme Model. . *Inorg. Chem.* **2017**, *56*, 7803-7810.
(28) Bohle, D. S.; Kosar, A. D.; Madsen., S. K. Propionic Acid Side Chain Hydrogen Bonding in the Malaria Pigment β-Hematin. . *Biochem. Biophys. Res. Commun.* **2002**, *294*, 132-135.
(29) Blauer, G.; Akkawi, M. Investigations of B- and beta-hematin. *Journal of inorganic biochemistry FIELD Publication Date:1997 May 1*, *66*, 145-152. FIELD Reference Number: FIELD Journal Code:7905788 FIELD Call Number:.
(30) Li, Y.; Zhang, L. In *Heme Biology*; Zhang, L., Ed.; World Scientific: New York, NY, 2011, p 161-196.
(31) Reedy, C. J.; Gibney, B. R. Heme Protein Assemblies. *Chem. Rev.* **2004**, *104*, 617-640.
(32) DiNello, R. K.; Chang, C. K. In *The Porphyrins*; Dolphin, D., Ed.; Wiley-Interscience: New York; Vol. 1, p 289-339.
(33) Portela, C.; Afonso, C. M. M.; Pinto, M. M. M.; Joao Ramos, M. Computational studies of new potential antimalarial compounds - Stereoelectronic complementarity with the receptor. *J. Comp.-Aid. Mole. Design* **2003**, *17*, 583-595.
(34) Gorka, A. P.; de Dios, A.; Roepe, P. D. Quinoline Drug-Heme Interactions and Implications for Antimalarial Cytostatic versus Cytocidal Activities. *J. Med. Chem.* **2013**, *56*, 5231-5246.
(35) Wicht, K. J.; Combrinck, J. M.; Smith, P. J.; Hunter, R.; Egan, T. J. Identification and SAR Evaluation of Hemozoin-Inhibiting Benzamides Active against Plasmodium falciparum. *J. Med. Chem.* **2016**, *59*, 6512-6530.
(36) Buller, R.; Peterson, M. L.; Almarsson, O.; Leiserowitz, L. Quinoline Binding Site on Malaria Pigment Crystal: A Rational Pathway for Antimalaria Drug Design. *Cryst. Grow. Des.* **2002**, *2*, 553-562.
(37) Durrant, M. C. A computational study of ligand binding affinities in iron(III) porphine and protoporphyrin IX complexes. *Dalton Trans* **2014**, *43*, 9754-9765.
(38) Kalani, K.; Cheema, H. S.; Tripathi, H.; Khan, F.; Daroker, M. P.; Srivastava, S. K. QSAR-guided semi-synthesis and in vitro validation of antiplasmodial activity in ursolic acid derivatives. *RSC Adv.* **2015**, *5*, 32133-32143.
(39) Roberts, L. Drug-resistant malaria advances in Mekong. *Science* **2017**, *358*, 155-156.
(40) Coelho, A. A., TOPAS-Academic Version 6 Technical Reference 2016, available at http://www.topas-academic.net.
(41) Frisch, M. J.; Trucks, G. W.; Schlegel, H. B.; Scuseria, G. E.; Robb, M. A.; Cheeseman, J. R.; Zakrzewski, V. G.; Montgomery, J. A.; Stratmann, R. E.; Burant, J. C.; Dapprich, S.; Millam, J. M.; Daniels, A. D.; Kudin, K. N.; Strain, M. C.; Farkas, O.; Tomasi, J.; Barone, V.; Cossi, M.; Cammi, R.; Mennucci, B.; Pomelli, C.; Adamo, C.; Clifford, S.; Ochterski, J.; Petersson, J. A.; Ayala, P. Y.; Cui, Q.; Morokuma, K.; Malick, D. K.; Rabuck, A. D.; Raghavachari, K.; Foresman, J. B.; Cioslowski, J.; Ortiz, J. V.; Stefanov, B. B.; Liu, G.; Liashenko, A.; Piskorz, P.; Kamaromi, I.; Gomperts, R.; Martin, R. L.; Fox, D. J.; Keith, T.; Al-Laham, M. A.; Peng, C. Y.; Nanayakkara, A.; Gonzalez, C.; Challacombe, M.; Gill, P. M. W.; Johnson, B. G.; Chen, W.; Wong, M. W.; Andres, J. L.; Head-Gordon, M.; Replogle, E. S.; Pople, J. A., Gaussian 98.1998,
(42) Roothaan, C. C. *J. Rev. Mod. Phys.* **1951**, *23*, 69-89.

10.1002/chem.201805116

Graphical Abstract:

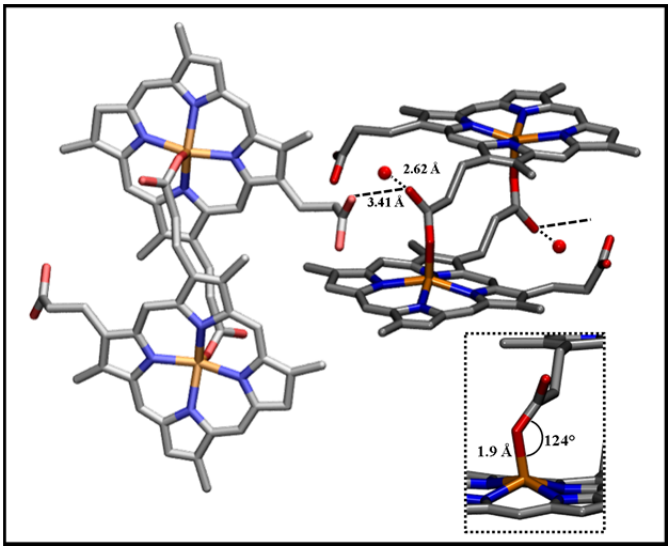

A new structural motif for heme dimerization relevant to malarial heme processing and aggregation has been found for the iron(deuteroprophyrin) dimer.

Abstract:

Treating deuterohemin, chloro(deuteroprophyrinato)iron(III), with a non-coordinating base in DMSO and methanol allows for the isolation of [(deuteroporphyrinato)iron(III)]$_2$, deuterohematin anhydride, DHA, an analog of malaria pigment, the natural product of heme detoxification by malaria. The structure of DHA from this solvent system has been solved by X-ray powder diffraction and displays many similarities and important structural differences with malaria pigment. Most notably the two waters sit in two notches created by the propionate sidechains and stabilize a markedly bent propionate coordinate with a long Fe-O bond and the formation of carboxylate cluster associated with the waters. Together these account for its increased solubility and more open structure with an increased porphyrin-porphyrin separation.

10.1002/chem.201805116

This structure also accounts for the strong IR bands at 1587 cm^{-1} which are also found in many amorphous preparations of synthetic malaria pigment and it is proposed that stabilizing these structures may be new antimalarial drug targets. The important role for the vinyl substituents in this biochemistry is further demonstrated by the structure of deuterohemin from single crystal X-ray diffraction.